NJC

RSC Publishing

PAPER

View Article Online
View Journal | View Issue

Cite this: *New J. Chem.*, 2013, **37**, 1122

Thymidine-based amphiphiles and their bonding to DNA†

Delin Pan, Chen Tang, Xinmeng Fan, Yating Li, Xiantao Yang, Hongwei Jin, Zhu Guan, Zhenjun Yang* and Lihe Zhang

Received (in Montpellier, France) 22nd November 2012, Accepted 22nd January 2013

DOI: 10.1039/c3nj41062e

www.rsc.org/njc

To develop non-cationic vectors for gene delivery, a novel class of thymidine-based amphiphiles have been constructed. These molecules showed good biocompatibility. Their complexation with polyadenylic acid through hydrogen bonding and π–π stacking interaction was demonstrated by gel electrophoresis, capillary electrophoresis, transmission electronic microscopy (TEM) and molecular dynamics simulation. It was also found that their biocompatibility and binding ability with DNA varied inversely with the length of the alkyl chains.

Introduction

Gene therapy has gained significant attention as a potential method for treatment of both acquired and inherited diseases.[1,2] Naked nucleic acids are easily degraded when used either *in vitro* or *in vivo*, so vectors are employed in many methods to protect nucleic acids and deliver them to targeted cells. Viruses are efficient vectors for transportation of genes. However, clinical applications of these vectors are restricted due to their toxicity and immunogenicity.[3] Consequently, various kinds of synthetic nonviral vectors have been investigated, including cationic lipids, dendrimers, peptides, and polymers.[4] A large number of novel cationic lipids have been designed and assayed in transfection protocols, where nucleic acids bind to cationic liposomes because of the charge interaction between the negatively charged phosphate backbone of DNA and cationic headgroup of the lipid.[5] Cationic liposomes are of great interest as gene transfection agents, but there are still significant shortcomings because of their cytotoxicity and the possible binding to serum proteins, mostly negatively charged at physiological pH.[6] Although studies have exploited the fact that divalent cations can mediate the interaction between DNA and zwitterionic natural phospholipids (*i.e.*, lecithins) leading to the formation of Ca-mediated lipoplexes,[7,8] to the best of our knowledge there has been no report of natural or anionic lipids used for gene delivery.

Nucleoside-based amphiphiles, which have a double functionality based on the combination of nucleic acids and lipid characteristics, have attracted much attention in the last decades.[9–12] These molecules constructed a large variety of supramolecular systems.[13–18] Interestingly, lipoplexes only stabilized *via* base pairing interaction could be obtained by molecular recognition between micellar systems made of short chain nucleolipids and complementary polynucleotides.[19,20] Besides, a thymine–lipoamino acid conjugate was reported, which could form complexes with single-stranded DNA by hydrogen bond networks in aqueous media,[21] and a class of hydrogelators containing nucleobases were also reported to be able to bind and deliver nucleic acids.[22] These studies have opened the door for the design of novel classes of non-cationic vectors for gene delivery, and the investigation of non-charge interactions between nucleoside-based amphiphiles and nucleic acids is still important for continued advancements in this area.

3′-*O*-Alkyl nucleotide was reported by Barthélémy and co-workers many years ago, and has alkyl chain lengths of 16 or 20 carbon atoms (C20-3′TMP and C20-3′AMP, Fig. 1a and b).[23,24] The authors investigated their supramolecular assemblies in aqueous media and on a graphite surface. Results showed that these nucleotide amphiphiles spontaneously assembled to many nano-structures, but the application of them in gene delivery was not investigated. Our group has been studying novel gene delivery systems for many years.[25–27] We considered the potential application of 3′-*O*-alkyl nucleotide as a nonviral vector for genes, and the report[20] that short-chain nucleolipids realized molecular recognition with polynucleotides encouraged us to construct short-chain 3′-*O*-alkyl nucleotides ($TMPC_8$, $TMPC_{12}$ and $TMPC_{16}$, Fig. 1c–e), and to investigate

State Key Laboratory of Natural and Biomimetic Drugs, School of Pharmaceutical Sciences, Peking University, Xue Yuan Road 38, Beijing 100191, China. E-mail: yangzj@bjmu.edu.cn; Fax: +86 10-8280-2503; Tel: +86 10-8280-2503

† Electronic supplementary information (ESI) available: Synthetic procedures and characterization data, ^1H, ^{13}C and ^{31}P NMR spectra, gel electrophoresis images. See DOI: 10.1039/c3nj41062e

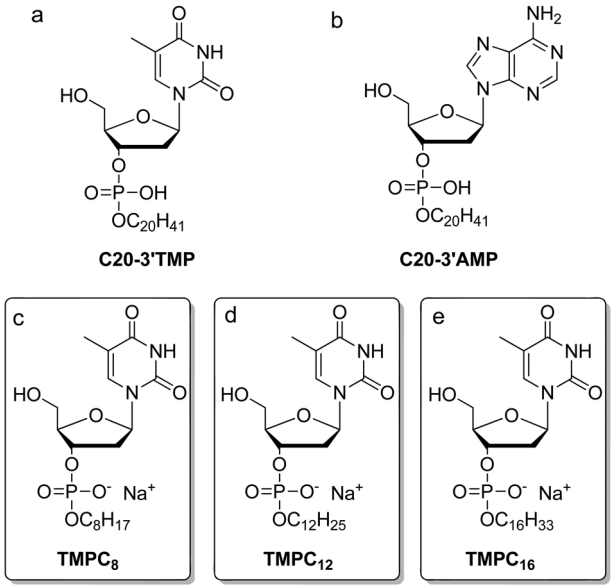

Fig. 1 Chemical structures of nucleoside-based amphiphiles.

their complexation with DNA in aqueous media. Sodium salts of these nucleotides were designed to increase their water solubility.

Experimental

Synthesis

Reagents were purchased in analytical grade or higher purity from Sigma-Aldrich or Alfa Aesar. Unless otherwise noted, materials obtained from commercial suppliers were used without further purification. ^{1}H, ^{13}C, and ^{31}P NMR were recorded on a Bruker AVIII-400 spectrometer. Infrared (IR) spectra were obtained using a Spectrum One Fourier transform infrared (FT-IR) spectrometer (Nexus 470, Thermo Nicolet Co. Ltd.). Mass spectra were recorded using a Xevo G2 Q-TOF spectrometer. High-resolution mass spectra were recorded using a APEX IV FT-MS (7.0T) spectrometer.

General procedure for the synthesis of 3′-*O*-alkyl nucleotide. A solution of 3′-phosphoramidites-5′-protected thymidine (compound **1**, 750 mg, 1 mmol) and 1*H*-tetrazolium (70 mg) in 15 mL anhydrous acetonitrile was cooled to 0 °C. Aliphatic alcohol (2 mmol) was added to this solution. The reaction mixture was stirred for 2 h at room temperature under argon. After that, solvent was removed under vacuum. The residue was re-dissolved in CH_2Cl_2 (15 mL), and *t*-BuOOH (0.2 mL) was added to this solution. After stirring for 30 min, solvent was removed under vacuum, and the residue was re-dissolved in $CHCl_2CO_2H$–CH_2Cl_2 (3%, 20 mL). The reaction mixture was stirred for 30 min at room temperature, and purified by column chromatography over silica with dichloromethane/methanol (20/1) as the eluting solvent to give compound **2**. 200 mg of compound **2** was dissolved in methanol–ammonia (20 mL) and stirred at room temperature for 2 h. After that, the solvent was evaporated to give a yellow residue. The residue was purified by column chromatography (Sephadex LH 20, DCM/MeOH 1/1), and applied to a column of Dowex 50 WX4 (200–400 mesh) to give the desired product.

Biocompatibility

Cell viability and proliferation were measured with a Cell Counting KIT-8 (CCK-8, Dojindo, www.dojindo.cn). This system consisted of WST-8 (2-[2-methoxy-4-nitrophenyl]-3-[4-nitrophenyl]-5-[2,4-disulfophenyl]-2*H*-tetrazolium, monosodium salt) that produced a water-soluble formazan dye upon bioreduction in the presence of an electron carrier.[28] WST-8 is reduced by dehydrogenase in cells to give a yellow product (formazan), which is soluble in the tissue culture medium. The amount of the formazan dye generated by the activity of dehydrogenases in cells is directly proportional to the number of living cells. 8000 cells (HEK293) were seeded on a 96-well plate with DMEM + 10% FBS and incubated at 37 °C and humidified 5% CO_2 for 18–24 hours until confluency reached ~70%. Nucleotide amphiphiles at different concentrations were added, and plates were incubated for another 24 h. Then 10 microliters of thawed CCK-8 solution was added to each well. Plates were incubated for 2 h at the same incubator conditions, after which the absorbance was read at 450 nm with a reference wavelength of 600 nm. After deducting the absorbance of nucleotide amphiphiles themselves (plates without cell), cell number was correlated to optical density (OD). Cell viability was calculated as:

$$\text{cell viability} = (OD_{450(\text{sample})}/OD_{450(\text{control})}) \times 100\%$$

where $OD_{450(\text{sample})}$ is the absorbance at 450 nm of cells added with nucleotide amphiphiles, and $OD_{450(\text{control})}$ is the absorbance at 450 nm of the negative control.

Gel electrophoresis

Nucleotide amphiphile was mixed with polyadenylic acid (polyA, 20 bps) at a base ratio of 10/1, and the sample was heated at 60 °C and equilibrated at 4 °C for about a week (annealing). A fraction (4 nmol of nucleotide amphiphile) of the sample was analyzed on a TBE-buffered, 40% polyacrylamide gel. The gel was stained using SYBR Gold (Invitrogen, Carlsbad, California) for 15 min and then visualized using a UV transluminator and CCD camera. UV images and relative quantification analysis were carried out using the ChemiDoc XRS System (Bio-RAD, USA).

Capillary electrophoresis

Experiments were performed on a Beckman Proteomelab™ PA800 system (Beckman Coulter, Fullerton, CA, USA) equipped with UV and LIF detector as well as the 32 Karat™ software (Beckman Coulter). A capillary tube (Yongnian Optical Fiber, Hebei, China) with i.d. of 100 μm was used. The total and effective lengths of the capillary were 30.2 and 20 cm, respectively. Before using, the new capillaries were rinsed with NaOH solution (0.1 mol L^{-1}) for 20 min, and subsequently with deionized water for 5 min.

PEG of molecular weight 35 000 (PEG 35 000) was purchased from Fluka (Buchs, Switzerland). Acrylamide, Tris base, TEMED (99%), 3-(methacryloyloxy)propyltrimethoxysilane (γ-MAPS, 98%)

and ammonium persulfate (APS, >98%) were obtained from Sigma (St Louis, MO, USA). Other reagents were all of analytical grade and from Beijing Chemical Reagent Factory (Beijing, China).

Bare fused-silica capillaries were permanently coated with polyacrylamide according to the method described in ref. 29, in which 4% linear polyacrylamide (LPA) and γ-methacryloxypropyltrimethoxysilane were used. Running buffer was prepared by dissolution of Tris, boric acid and EDTA-2Na (TBE) to the appropriate concentrations. Prior to use, the buffer was degassed for 10 min in an ultrasonic bath and filtered through a 0.45 μm filter. Polymer solution was prepared by dissolution of PEG 35 000 in the above corresponding buffer to the appropriate concentrations, followed by stirring and degassing before use. Samples were introduced by electrokinetic mode at −10 kV for 5 s. The UV detection wavelength was 254 nm. The best separation of the samples was obtained at PEG concentration of 20% and TBE concentration of 25 mmol L^{-1} (pH 8.0), and the optimal separation voltage was −20 kV.

TEM image

To prepare TEM sample, a drop of the aqueous solution (100 μM) of was allowed to air-dry onto a formvar-carbon-coated 230 mesh copper grid. The TEM experiments were performed using a Philips Tacnai G2 20 S-TWIN microscope operating at 200 kV.

Molecular dynamics (MD) simulation

MD simulation was performed with AMBER 11 molecular simulation package.[30] The AMBER99 force field was used to describe the $TMPC_{12}$-polyA complex. To obtain molecular mechanical parameters for the $TMPC_{12}$, *ab initio* quantum chemical methods were employed using the Gaussian 09 program.[31] The geometry was fully optimized and then the electrostatic potentials around them were determined at the HF/6-31G* level of theory. The RESP strategy[32] was used to obtain the partial atomic charges.

The starting model of $TMPC_{12}$–polyA complex was built using Discovery Studio 2.5 software. The model was solvated in TIP3P water using a octahedral box, which extended 8 Å away from any solute atom. To neutralize the negative charges of simulated molecules, Na^+ counterions were placed next to each phosphate group.

Molecular dynamics (MD) simulation was carried out by using the SANDER module of AMBER 11. The calculations began with 500 steps of steepest descent followed by 500 steps of conjugate gradient minimization with a large constraint of 500 kcal mol^{-1} $Å^{-2}$ on the $TMPC_{12}$–polyA complex. Then 1000 steps of steepest descent followed by 1500 steps of conjugate gradient minimization with no restraints on the $TMPC_{12}$-polyA complex were performed. Subsequently, after 20 ps of MD, during which the temperature was slowly raised from 0 to 300 K with weak (10 kcal mol^{-1} $Å^{-2}$) restraints on the $TMPC_{12}$–polyA complex, the final unrestrained production simulations of 3.0 ns for the molecule was carried out at constant pressure (1 atm) and temperature (300 K). In the entire simulation, SHAKE was applied to all hydrogen atoms. Periodic boundary conditions with minimum image conventions were applied to calculate the nonbonded interactions. A cutoff of 10 Å was used for the Lennard–Jones interactions. The final structure of $TMPC_{12}$–polyA complex was produced from the 1000 steps of minimized averaged structure of the last 2.0 ns of MD.

Results and discussion

Commercially available 3′-phosphoramidites-5′-protected thymidine (**1**) was used as the starting material, and the synthetic approach was somewhat different to the literature (Scheme 1).[23] Intermediate **2** was obtained after the reaction of compound **1** with aliphatic alcohol, deprotection and oxidation in one pot. This intermediate was reacted in methanol–ammonia solution, and applied to an ion exchange column to give the desired product.

To verify the biocompatibility of nucleotide amphiphiles, we added $TMPC_8$, $TMPC_{12}$ or $TMPC_{16}$ to the culture of Human Embryonic Kidney 293 cells, and cell proliferation was measured with a Cell Counting KIT-8 (CCK-8). As shown in Fig. 2, after being incubated with $TMPC_8$ or $TMPC_{12}$ at 100 μM for 24 h, the viability of HEK 293 cells remained at nearly 100%, indicating that these molecules are fully biocompatible. However, $TMPC_{16}$ exhibited bad biocompatibility, and this result also encouraged us to investigate the biological application of short chain 3′-*O*-alkyl nucleotides.

In order to determine whether the nucleotide amphiphiles bind nucleic acids, we performed gel electrophoresis (GE) assay with polyadenylic acid (polyA, 20 bps) as a model system. $TMPC_8$, $TMPC_{12}$ or $TMPC_{16}$ was mixed with polyA at a base ratio of 10/1, and the samples were heated at 60 °C and equilibrated at 4 °C for about a week (annealing). The annealing treatment was also performed on the aqueous dispersions of $TMPC_8$, $TMPC_{12}$, $TMPC_{16}$ and polyA. After that, the samples were run on non-denaturing polyacrylamide gel and stained by SYBR Gold,[33] a commercially available nucleic acid gel stain. In Fig. 3, the bright band for the free polyA in column (a) disappeared entirely for the $TMPC_8$–polyA mixture (column b), darkened obviously for the $TMPC_{12}$–polyA mixture (column d), but changed insignificantly for the $TMPC_{16}$–polyA mixture (column f). Columns c and e do not contain any polyA and as expected show no indication of the presence of SYBR Gold. These results indicated that a full complexation occurred for

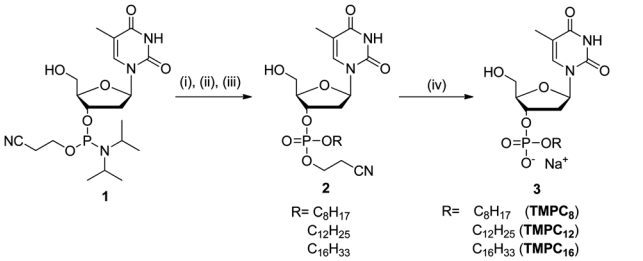

Scheme 1 (i) ROH, 1*H*-tetrazolium, anhydrous acetonitrile, 0 °C to r.t., argon, 2 h; (ii) *t*-BuOOH, CH_2Cl_2, r.t., 30 min; (iii) $CHCl_2CO_2H$–CH_2Cl_2 (3%), 30 min; (iv) NH_3–MeOH, r.t., 2 h, Dowex 50 WX4 (200–400 mesh).

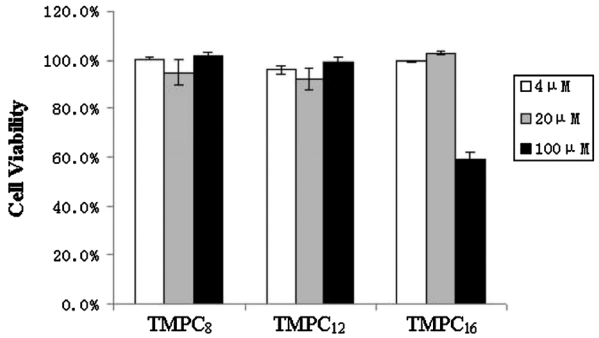

Fig. 2 HEK 293 cell viability test for 24 h of $TMPC_8$, $TMPC_{12}$ and $TMPC_{16}$.

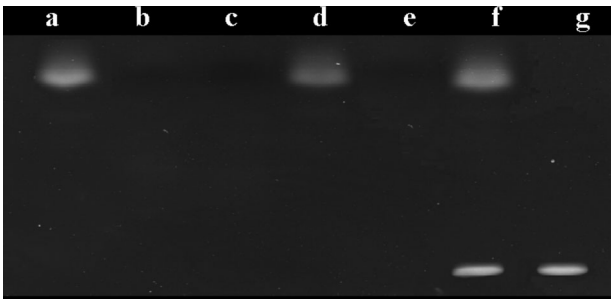

Fig. 3 Electrophoretic mobility of (a) polyA; (b) $TMPC_8$–polyA (10/1); (c) $TMPC_8$; (d) $TMPC_{12}$–polyA (10/1); (e) $TMPC_{12}$; (f) $TMPC_{16}$–polyA (10/1) and (g) $TMPC_{16}$, respectively.

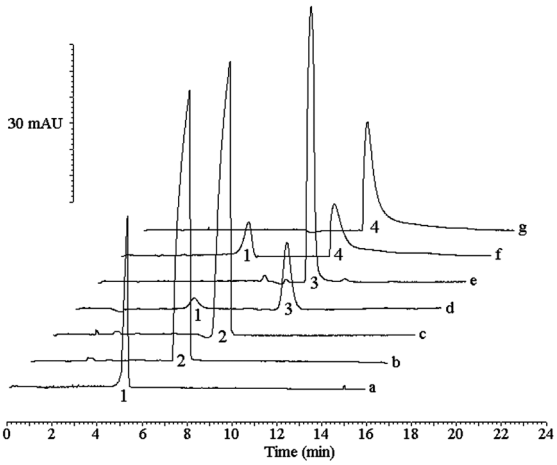

Fig. 4 Electropherograms of (a) polyA; (b) $TMPC_8$–polyA (10/1), (c) $TMPC_8$; (d) $TMPC_{12}$–polyA (10/1), (e) $TMPC_{12}$; (f) $TMPC_{16}$–polyA (10/1) and (g) $TMPC_{16}$, respectively. The separation system is described in the ESI.† The marked peaks 1, 2, 3 and 4 represent polyA, $TMPC_8$, $TMPC_{12}$ and $TMPC_{16}$, respectively.

Table 1 Relative peak area of remained polyA and nucleotide amphiphiles after complexation[a]

	$TMPC_8$–polyA	$TMPC_{12}$–polyA	$TMPC_{16}$–polyA
polyA	0	0.15	0.44
NA[b]	0.33	0.31	0.52

[a] Peak areas relative to corresponding external standards (Fig. 3; peak 1 of spectrum a, peak 2 of spectrum c, peak 3 of spectrum e, and peak 4 of spectrum g were used as external standards, respectively). [b] NA = nucleotide amphiphile.

the $TMPC_8$–polyA mixture, and the complexation decreases with the growth of the alkyl chain of nucleotide amphiphile. However, the bands of the complexes of polyA with nucleotide amphiphiles were not detected in this experiment. FAM (5-carboxyfluorescein)-labeled polyA was used to track the complex formation (see the ESI†). Based on the experimental results, we believe that the complexes have dispersed in the column and the concentration was at too low a level to be detected. Interestingly, it was observed that $TMPC_{16}$ was also stained by SYBR Gold (Fig. 3, columns f & g), indicating that its supramolecular assembly resembled DNA in architecture. It was supposed that the tendency of self-assembly inhibited the complexation of $TMPC_{16}$ with DNA.

As a more sensitive analysis tool, capillary electrophoresis (CE) was also used to investigate the complexation of nucleotide amphiphiles with polyA. Samples were prepared the same way as GE assay, and performed on a no-gel CE.[34] Products were qualitatively determined by contrasting with standard sample, and quantitatively determined by calculating the peak areas. As shown in Fig. 4, after the addition of $TMPC_8$, $TMPC_{12}$ or $TMPC_{16}$, the peak of polyA disappeared or decreased correspondingly. Relative peak areas were given in Table 1, which suggested that $TMPC_8$ has fully bound the polynucleotides, $TMPC_{12}$ has bound most of the polynucleotides, and $TMPC_{16}$ has bound only part of the polynucleotides. This result coincided with GE assay, indicating that the complexation decreases with the growth of the alkyl chain of nucleotide amphiphile. Unfortunately, the complexes of polyA with nucleotide amphiphiles were not detected in these electropherograms, either.

The supramolecular assemblies of $TMPC_8$, $TMPC_{12}$ and $TMPC_{16}$ were investigated by transmission electron microscopy (TEM). Ribbon-like structures were observed in the aqueous dispersion of $TMPC_{16}$, as reported by Barthélémy and co-workers (Fig. 5a).[23] However, similar structures were not observed in aqueous dispersions of short-chain nucleotide amphiphiles. As shown in Fig. 5b, $TMPC_{12}$ formed conglutinant vesicles at a dimension of approximately 30 nm in aqueous solution. It was supposed that the different hydrophobicity of alkyl chains, and the different phase transition temperatures, caused the diversity on supramolecular assemblies of $TMPC_{16}$ and $TMPC_{12}$. In addition, a supramolecular structure was not observed in the aqueous dispersion of $TMPC_8$, and that was because $TMPC_8$ is completely soluble in aqueous media to form a true solution. Actually, it has been observed that the sodium salt of $TMPC_8$ is highly hygroscopic in atmospheric conditions.

To investigate the supramolecular structure variation of $TMPC_{16}$ and $TMPC_{12}$ after the addition of polyA, TEM images of these complexes were observed. Ribbon-like structures were also observed in $TMPC_{16}$–polyA mixture solution (Fig. 5c), which was almost the same as the TEM image of $TMPC_{16}$ aqueous solution. This result coincided with GE and CE

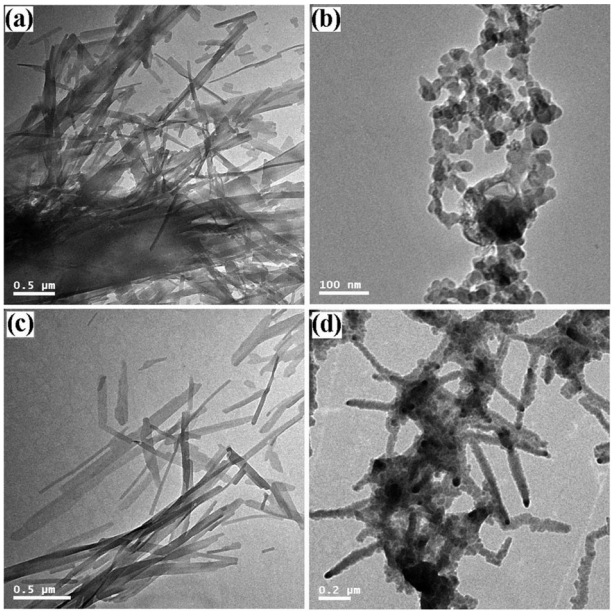

Fig. 5 TEM image of (a) $TMPC_{16}$ (bar = 500 nm), (b) $TMPC_{12}$ (bar = 100 nm), (c) $TMPC_{16}$–polyA mixture (bar = 500 nm) and (d) $TMPC_{12}$–polyA mixture (bar = 200 nm) in aqueous solution.

experiments, indicating a low binding interaction between $TMPC_{16}$ and poly A.

On the other hand, the TEM image of $TMPC_{12}$ changed dramatically after the addition of polyA. As shown in Fig. 5d, "worm"-like structures were observed in the mixed solution of $TMPC_{12}$ and polyA, in contrast to the vesicle structures of $TMPC_{12}$ aqueous solution. This variation on supramolecular architecture indicated the binding of nucleotide amphiphiles with polyA.

Molecular dynamics simulation was used to study the thermodynamic stability of $TMPC_{12}$–polyA complex. A 3.0 ns MD simulation of the complex led to a stable trajectory of geometry and energy terms. The calculated root-mean-square deviation (RMSD) values stabilized and remained stable during the last 2.0 ns period of simulation. As shown in Fig. 6a and b, calculation results demonstrated a dsDNA-like complex in aqueous solution based on π–π stacking and Watson–Crick base-pairing interactions. Taking the 10th deoxyadenosine (from the 5′ end) and the corresponding $TMPC_{12}$ molecule bound to it for an example, the length of N–H and O–H hydrogen bonds were respectively 1.885 Å and 1.852 Å (Fig. 6c), which are close to those in the canonical Watson–Crick base-pairing modes (1.832 Å and 1.930 Å, respectively).[35] However, for the 20th deoxyadenosine and the corresponding $TMPC_{12}$ molecule, the distances are much longer (Fig. 6d, 4.469 and 3.790 Å for N–H and O–H, respectively) because of edge effects, which decrease the stability of the complex.

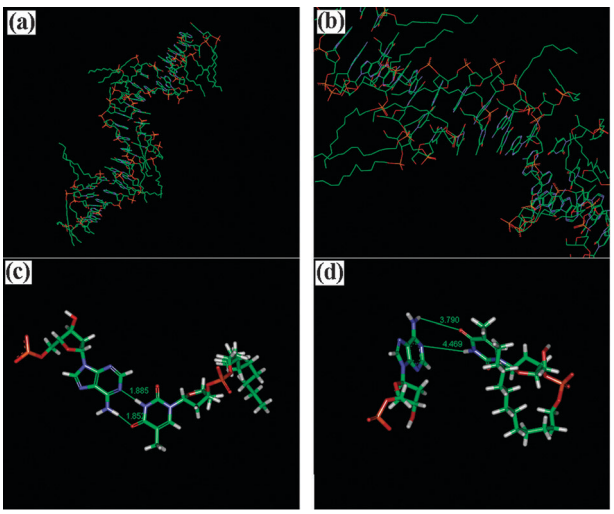

Fig. 6 (a) and (b) Molecular dynamics simulation result of $TMPC_{12}$–polyA complex. Simulation structures of (c) the 10th and (d) 20th deoxyadenosines (from the 5′-end) and the corresponding $TMPC_{12}$ molecules binding to them.

Conclusions

In conclusion, we have developed a novel class of thymidine-based amphiphiles, and investigated their complexation with single-stranded DNA through hydrogen bonding and π–π stacking interactions. Experimental results from gel electrophoresis, capillary electrophoresis, transmission electron microscopy and molecular dynamics simulation supported the binding of these nucleotide amphiphiles with polyadenylic acid. Furthermore, it was found that their biocompatibility and binding ability with DNA varied inversely with the length of the alkyl chains. It is obvious that these molecules are negatively charged, and this research provided further evidence for the use of non-cationic interactions to manipulate DNA. The development of amphiphiles possessing affinity to DNA through more specific interactions, as opposed to more general electrostatic forces, will be a benefit for the design of novel classes of non-viral carriers for gene delivery. Further study on the application of these amphiphiles in gene delivery is ongoing in this laboratory.

Acknowledgements

This research was supported by Ministry of Science and Technology of China (No. 2012CB720604) and NNSFC (No. 20932001), which are gratefully acknowledged. The authors thank Prof. Dr Yu Liu, Prof. Dr Yong Chen, Dr Ying-Ming Zhang and Yang Yang of Nankai University for their advice and help in this study.

Notes and references

1 R. A. Morgan and W. F. Anderson, *Annu. Rev. Biochem.*, 1993, **62**, 191–217.
2 R. I. Mahato and S. W. Kim, *Pharmaceutical Perspectives of Nucleic Acid-Based Therapeutics*, Taylor and Francis, London and New York, 2002.
3 E. Marshall, *Science*, 2000, **287**, 565–567.
4 M. A. Mintzer and E. E. Simanek, *Chem. Rev.*, 2009, **109**, 259–302.

5 D. D. Lasic, *Liposomes in Gene Delivery*, CRC Press, New York, 1997.
6 P. R. Dash, M. L. Read, L. B. Barrett, M. A. Wolfert and L. W. Seymour, *Gene Ther.*, 1999, **6**, 643–650.
7 H. Liang, D. Harries and G. C. L. Wong, *Proc. Natl. Acad. Sci. U. S. A.*, 2005, **102**, 11173–11178.
8 J. J. McManus, O. J. Radler, A. Kenneth and A. Dawson, *J. Am. Chem. Soc.*, 2004, **126**, 15966–15967.
9 P. Barthélémy, *C. R. Chim.*, 2009, **12**, 171–179.
10 H. Rosemeyer, *Chem. Biodiversity*, 2005, **2**, 977–1062.
11 A. Gissot, M. Camplo, M. W. Grinstaff and P. Barthélémy, *Org. Biomol. Chem.*, 2008, **6**, 1324–1333.
12 O. Kaczmarek, N. Brodersen, A. Bunge, L. Löser, D. Huster, A. Herrmann, A. Arbuzova and J. Liebscher, *Eur. J. Org. Chem.*, 2008, 1917–1928.
13 L. Moreau, P. Barthélémy, M. E. Maataoui and M. W. Grinstaff, *J. Am. Chem. Soc.*, 2004, **126**, 7533–7539.
14 L. Moreau, M. W. Grinstaff and P. Barthélémy, *Tetrahedron Lett.*, 2005, **46**, 1593–1596.
15 L. Moreau, N. Campins, M. W. Grinstaff and P. Barthélémy, *Tetrahedron Lett.*, 2006, **47**, 7117–7120.
16 C. Heiz, U. Rädler and P. L. Luisi, *J. Phys. Chem. B*, 1998, **102**, 8686–8691.
17 H. Yanagawa, Y. Ogawa, H. Furuta and K. Tsuno, *J. Am. Chem. Soc.*, 1989, **111**, 4567–4570.
18 Y. Itojima, Y. Ogawa, K. Tsuno, N. Handa and H. Yanagawa, *Biochemistry*, 1992, **31**, 4757–4765.
19 S. Milani, F. B. Bombelli, D. Berti and P. Baglioni, *J. Am. Chem. Soc.*, 2007, **129**, 11664–11665.
20 M. Banchelli, D. Berti and P. Baglioni, *Angew. Chem., Int. Ed.*, 2007, **46**, 3070–3073.
21 M. Skwarczynski, Z. M. Ziora, D. J. Coles, I.-C. Lin and I. Toth, *Chem. Commun.*, 2010, **46**, 3140–3142.
22 X. Li, Y. Kuang, J. Shi, Y. Gao, H.-C. Lin and B. Xu, *J. Am. Chem. Soc.*, 2011, **133**, 17513–17518.
23 N. Campins, P. Dieudonné, M. W. Grinstaff and P. Barthélémy, *New J. Chem.*, 2007, **31**, 1928–1934.
24 I. Bestel, N. Campins, A. Marchenko, D. Fichou, M. W. Grinstaff and P. Barthélémy, *J. Colloid Interface Sci.*, 2008, **323**, 435–440.
25 X. X. Li, L. R. Zhang, J. F. Lu, Y. Z. Chen, J. M. Min and L. H. Zhang, *Bioconjugate Chem.*, 2003, **14**, 153–157.
26 C. P. Chen, L. R. Zhang, Y. F. Peng, X. B. Wang, S. Q. Wang and L. H. Zhang, *Bioconjugate Chem.*, 2003, **14**, 532–538.
27 Y. Liu, X. F. Wang, Y. Chen, L. H. Zhang and Z. J. Yang, *Med. Chem. Commun.*, 2012, **3**, 506–511.
28 M. Ishiyama, H. Tominaga, M. Shiga, K. Sasamoto, Y. Ohkura and K. Ueno, *Biol. Pharm. Bull.*, 1996, **19**, 1518–1520.
29 S. Hjerten, *J. Chromatogr., A*, 1985, **347**, 191–198.
30 D. A. Case, T. A. Darden and T. E. Cheatham, *et al.*, *AMBER 11*, University of California, San Francisco, 2010.
31 M. J. Frisch, G. W. Trucks and H. B. Schlegel, *et al.*, *Gaussian 09, Revision A.1*, Gaussian, Inc, Wallingford CT, 2009.
32 C. I. Bayly, P. Cieplak, W. D. Cornell and P. A. Kollman, *J. Phys. Chem.*, 1993, **97**, 10269–10280.
33 R. S. Tuma, M. P. Beaudet, X. Jin, L. J. Jones, C.-Y. Cheung, S. Yue and V. L. Singer, *Anal. Biochem.*, 1999, **268**, 278–288.
34 W. Li, M. Cao, L. Pei, X. Ling, B. Li and Z. Yang, *Electrophoresis*, 2010, **31**, 507–511.
35 W. Saenger, *Principles of Nucleic Acid Structure*, Spring-Verlag, New York, 1984.